

Anderson Localization of Electrons in Dense ^4He Gas

P. W. Adams and M. A. Paalanen

AT&T Bell Laboratories, Murray Hill, New Jersey 07974

(Received 26 October 1987; revised manuscript received 20 May 1988)

The conductance of a dilute 2D electron gas on hydrogen is measured as a function of ambient ^4He gas density. At densities below $\approx 10^{20} \text{ cm}^{-3}$ the electron scattering rate is the sum of a classical term linear in ^4He density plus a ^4He -adsorbate-scattering term. Towards higher densities, however, the conductivity decreases exponentially which we attribute to strong localization of electrons below a threshold energy $E_c \gtrsim k_B T$. We present an estimate of E_c based on weak-localization theory and find good agreement with both our 2D data and the 3D mobility measurements in the literature. In 3D, the Ioffe-Regel criterion for localization is found to be $kl_0 = 2.5 \pm 0.5$.

PACS numbers: 73.20.Fz, 71.55.Jv

Electrons in dense ^4He gas represent an almost ideal system in which to study transport in a highly disordered media. Helium provides a short-range, well characterized localization potential whose fluctuations can easily exceed the average kinetic energy of the electrons.¹ The idea of one's using helium to reach this strongly disordered limit is not new and several elegant experiments have been performed showing substantial deviations from classical transport.²⁻⁴ These results have not, however, spurred much interest in the general solid-state community. One reason for this, we believe, is that there has been no clear quantitative connection made between the observed nonclassical transport properties of electrons in helium and what is known about transport in disordered metallic and semiconducting systems.⁵ With the recent development of quantum localization theory,⁶ it has now become possible to interpret electron transport in helium in more universal terms. In this Letter, we report a systematic investigation of the conductivity of a dilute two-dimensional electron gas on a solid hydrogen substrate as a function of ambient ^4He gas density. We analyze our data using the first-order single-electron weak-localization corrections to the conductivity and find evidence for a density-dependent strong-localization threshold that dominates the conductivity at high densities.

The interaction of very low-energy electrons with helium gas is well characterized by an effective optical scattering potential $\Delta V_0 = (\hbar^2/m_e)2\pi\Delta n_g a$, where $a \approx 6 \times 10^{-2} \text{ nm}$ is the electron-helium scattering length and Δn_g represents the density fluctuations in the gas.² In a nearly ideal gas like ^4He the density fluctuations are well known and in Born approximation^{2,7} the 3D scattering rate is

$$\tau_0^{-1} = \left(\frac{2E}{m_e} \right)^{1/2} \frac{4\pi a^2 n_g}{1 + 2B_2 n_g}, \quad (1)$$

and in 2D

$$\tau_0^{-1} = \frac{3\pi^2 \hbar a^2 n_g}{2m_e \langle z \rangle (1 + 2B_2 n_g)}. \quad (2)$$

In Eq. (2) $\langle z \rangle$, the average extent of the electron wave function above the H_2 surface,⁸ is $\approx 1.7 \text{ nm}$ and in both equations B_2 , the second virial coefficient of ^4He gas, takes into account the slight deviations of ^4He from the ideal gas behavior. At low ^4He densities the above classical scattering rates are proportional to n_g and one obtains the expected n_g^{-1} density dependences for both the mobility $\mu_0 = e\tau_0/m_e$ and conductivity $\sigma_0 = n_0 e^2 \tau_0/m_e$.

We have measured the conductivity and mobility for 2D electrons in dense ^4He gas with essentially the same experimental arrangement as first employed by Sommer and Tanner.^{3,9} Hydrogen crystals were formed on a 0.25-mm-thick sapphire disk onto which electrons were deposited. The coupling of the two-dimensional electron gas (2DEG) to a capacitive detector was measured by standard lock-in techniques, and the electron mobility μ , and conductivity σ , were determined by our applying a magnetic field, B , perpendicular to the surface and measuring the Drude resistivity, $\sigma^{-1}(B) = \sigma^{-1}[1 + (\mu B)^2]$ where $\sigma = \sigma_0$ and $\mu = \mu_0$ in the classical picture.

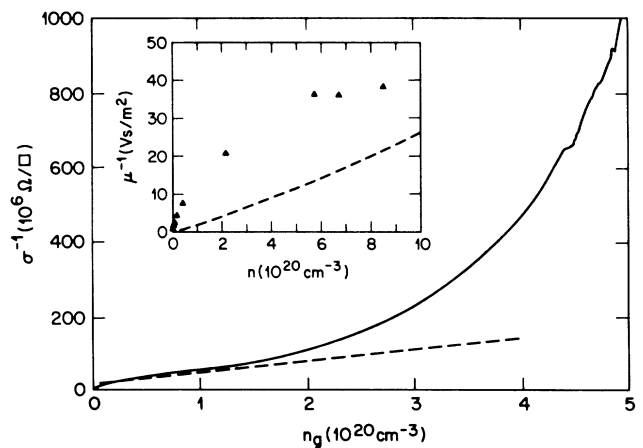


FIG. 1. Resistivity and inverse mobility of the 2DEG as functions of ^4He gas density n_g . Dashed lines are the slopes predicted with use of Eq. (2).

Shown in Fig. 1 is the resistivity σ^{-1} of the 2DEG as a function of gas density at 4.2 K. The electron density $n_0 \approx 10^8 \text{ cm}^{-2}$ was determined from the classical formula $n_0 = \sigma_0 / e\mu_0$ at the zero-gas-density limit. The small curvature near zero density represents scattering from the first ^4He submonolayer which is filled at $n_g \approx 2 \times 10^{19} \text{ cm}^{-3}$. As the ^4He density is further increased the gas-atom scattering begins to dominate and the conductivity becomes less sensitive to the surface interactions. The dashed line in Fig. 1 is the predicted slope from Eq. (2). Note the large deviation from linearity at densities $n_g > 10^{20} \text{ cm}^{-3}$ where the resistivity increases quickly and electrons become strongly localized. Similar behavior has been observed for 2DEG's on helium^{3,10,11} and on neon,¹² but no quantitative characterization of the data has been presented in these previous studies. In this work we have also determined the electron mobility from magnetoresistance at several ^4He densities and the inverse mobility, μ^{-1} , is plotted in the inset in Fig. 1. For comparison the dashed line is the classical prediction of Eq. (2). As in the case of σ^{-1} , the measured μ^{-1} is larger than the classical value; however, the difference is only about a factor of 2 at our highest densities and some of it is due to the surface scattering. This seems to indicate that the effective carrier density $n_{\text{eff}} = \sigma / e\mu$ rather than mobility μ vanishes in the strong-localization regime.

Levine and Sanders² were the first to observe large deviations from Eq. (1) in a nondegenerate 3D electron gas. They measured the electron mobility with a time-of-flight technique at $T \approx 4$ K and observed orders-of-magnitude lower mobilities than predicted by Eq. (1). They interpreted their observations as being evidence for the formation of an electron bubble state in the gas analogous to that observed in liquid ^4He . Later, Eggarter and Cohen¹³ developed a microscopic model of electron transport in helium where the anomalously low mobility was attributed to the formation of localized states. Though their percolation theory predated modern localization theory by some ten years, they were able to explain the data adequately using only two adjustable parameters. To the casual reader, however, the theory, which is based on several subtle and untestable assumptions, is not particularly transparent nor does it give a closed form to the density dependence of the mobility. Furthermore, the theory is limited to 3D transport and is hard to extend into 2D since it does not include the effects of inelastic scattering. In 2D inelastic effects are particularly important since all the single-electron eigenstates are localized at $T=0$ and finite-temperature conductivity appears through inelastic processes.

Equations (1) and (2) are lowest-order scattering results for plane-wave eigenstates and are not valid when the potential fluctuations exceed the electron kinetic energy $E \approx k_B T$.¹⁴ For sufficiently strong fluctuations the interference between multiple-scattering events has to be

taken into account. This is done by weak-localization theory, which predicts strong deviations from the classical results when $\hbar/\tau_0 \gtrsim k_B T$ ($k_{\text{th}} l_0 < 1$; k_{th} is thermal wave vector and l_0 the classical mean free path of the electron) and $\tau_\phi > \tau_0$ where τ_ϕ is the dephasing time. We have previously studied weak-localization effects for electrons on a bare H_2 surface and found, for example, the negative magnetoresistance peak predicted by this theory.⁹ On the basis of Eq. (2) we estimate that for our 2D electrons, $\hbar/\tau_0 \approx k_B T$ at $n_g \approx 10^{20} \text{ cm}^{-3}$, in agreement with the deviations observed in Fig. 1. The $\hbar/\tau_0 \gg k_B T$ ($kl_0 \sim 1$) regime (i.e., strong-localization regime) has remained inaccessible in photon-localization experiments¹⁵ and has not been systematically studied in degenerate electron systems where correlation effects are important. It is readily apparent from Eqs. (1) and (2) and Fig. 1 that helium gas provides a tunable and calculable random potential whose fluctuations can exceed the kinetic energy of the electrons at experimentally accessible densities.

In the presence of disorder, an electron's diffusivity is attenuated by coherent backscattering. To lowest order in $(kl_0)^{-1}$ the correction to the diffusivity in 3D is given by¹⁶

$$D(E) = \frac{2E\tau_0}{3m_e} \left\{ 1 - \frac{3\alpha}{(kl_0)^2} \left[1 - \left(\frac{\tau_0}{\tau_\phi} \right)^{1/2} \right] \right\}, \quad (3)$$

where α is an integration parameter of order 1. The 2D correction¹⁷ is

$$D(E) = \frac{E\tau_0}{m_e} \left[1 - \frac{\ln(\tau_\phi/\tau_0)}{\pi kl_0} \right]. \quad (4)$$

For $\tau_\phi \gg \tau_0$, Eqs. (3) and (4) predict a low diffusivity for electrons with $kl_0 \approx 1$ so that one should be careful to exclude carriers with $k \leq l_0^{-1}$ when calculating free-electron transport properties. For simplicity, we have neglected higher-order terms in $(kl_0)^{-1}$ as well as the possibility that l_0 , τ_0 , and τ_ϕ can be energy dependent beyond the first-order estimates of Eqs. (1) and (2). We have extrapolated the diffusivity to the limit $D(E_c) = 0$ using Eqs. (1)-(4) and then calculated the conductivity by integrating $D(E)$ over the Boltzmann distribution $f(E)$, $\sigma = \int_0^\infty D(E)n(E)f(E)dE$. When we take $D(E)$ to be zero for $E < E_c$ and $n(E)$ to be the free-electron density of states we get for both the 2D and 3D cases $\sigma = \sigma_0 \exp(-E_c/k_B T)$, where

$$E_c^{3D} = \alpha \frac{24\pi^2 \hbar^2 a^4 n_g^2}{m_e (1 + 2B_2 n_g)^2} \left[1 - \left(\frac{\tau_0}{\tau_\phi} \right)^{1/2} \right] \quad (5)$$

and

$$E_c^{2D} = \frac{3\pi \hbar^2 a^2 \ln(\tau_\phi/\tau_0) n_g}{4m_e \langle z \rangle (1 + 2B_2 n_g)}. \quad (6)$$

Notice that $E_c^{3D} \propto n_g^2$ but $E_c^{2D} \propto n_g$. Strictly speaking

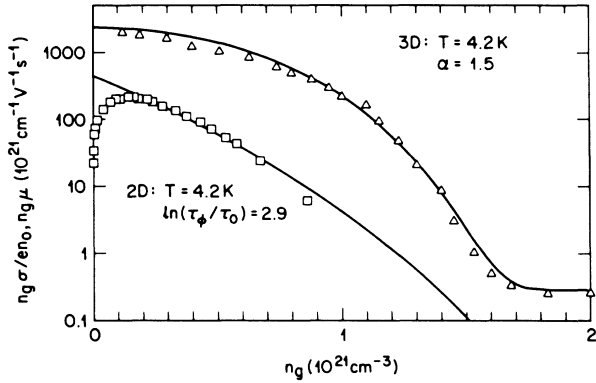


FIG. 2. The normalized conductivity (mobility) times density n_g as functions of n_g . The squares are the author's 2D data. The triangles are the 3D data from Ref. 4. The solid lines are best fits by Eqs. (5) and (6).

there is no mobility threshold in 2D at $T=0$ since all the electron eigenstates are localized. At finite temperature, however, effective threshold appears when the localization length, $l_{LOC} = l_0 \exp(kl_0)$ becomes less than the inelastic scattering length. Our model implicitly assumes in a statistical sense that the conductivity decrease is due to a vanishing number of mobile electrons $n_{eff} = n_0 \times \exp(-E_c/k_B T)$ in the $E > E_c$ tail of the Boltzmann distribution. We argue without rigorous proof that the nonvanishing mobility μ in Fig. 1, measured from the magnetoresistance, represents the average mobility of the electrons above the threshold E_c . This is to be contrasted with the typical time-of-flight measurements used to obtain 3D mobilities. In these experiments a time-averaged mobility is obtained which is essentially the average mobility of all the electrons over the whole Boltzmann distribution. Basically a single electron undergoes, during its flight time, many inelastic collisions probing the whole energy scale with a Boltzmann weighting factor. Therefore in 3D the measured mobility, $\mu = \mu_0 \exp(E_c^{3D}/k_B T)$, is analogous to our conductivity measurements.

We have tested the above ideas in Fig. 2 by plotting on a semilogarithmic scale both $n_g \sigma / en_0$ for our 2D data and $n_g \mu$ for the 3D data from Ref. 4, as functions of density n_g . Both of these data sets deviate strongly from the classical predictions of $n_g \sigma$ and $n_g \mu$, which are independent of n_g . Moreover, even though the 2D and 3D density ranges do not entirely overlap,¹⁸ we believe that there is clear dimensionality signature in these results. The solid lines in Fig. 2 are the best fits of the formulas $\sigma = \sigma_0 \exp(-E_c^{2D}/k_B T)$ and $\mu = \mu_0 \exp(-E_c^{3D}/k_B T)$ with use of Eqs. (5) and (6) for E_c . In the 3D case, $\tau_0/\tau_\phi \approx (m_e/M_{He})^{1/2}$ is small and thus the cutoff parameter α is the only adjustable parameter. With a reasonable value of $\alpha = 1.5$ we get a good fit to the data, comparable to those obtained by Eggarter and Cohen. In the 2D data the deviations at small gas densities are due to

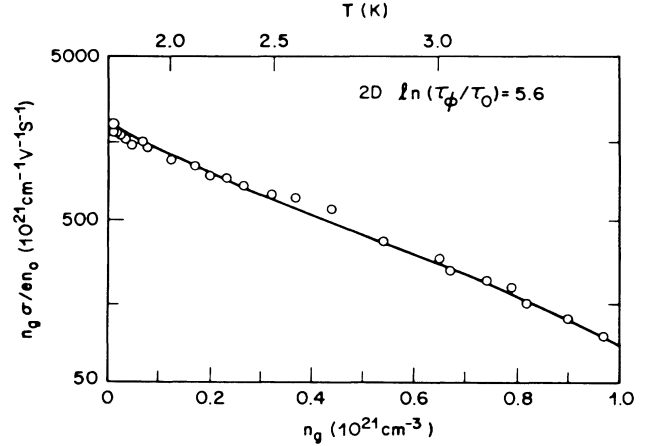


FIG. 3. The normalized conductivity times n_g as a function of n_g for electrons on ^4He from Ref. 3. The solid line is the best fit by Eq. (6) with $\langle z \rangle_{He} = 7.6$ nm.

the additional surface scattering, which is not included in the present theory. The best value of τ_ϕ obtained from the 2D fit is less than the 3D inelastic time $\approx (M_{He}/m_e)^{1/2} \tau_0$ but is in good agreement with values obtained from our low-field magnetoresistance measurements^{9,19} at $n_g \geq 5 \times 10^{20} \text{ cm}^{-3}$. We believe that the increased 2D dephasing was due to the configuration dephasing of ^4He atoms moving perpendicular to the surface.

Since E_c^{2D} is proportional to $\langle z \rangle^{-1}$ it is a useful test of the theory to fit conductivity measurements on helium where $\langle z \rangle_{He} \approx 4.5 \langle z \rangle_{H_2}$. Shown in Fig. 3 are the data of Sommer and Tanner^{3,20} for electrons on bulk helium. Again, the classical density dependence has been factored out and the temperature dependence of B_2 has been included. Note that the anomalous low- n_g behavior is not present in these data as there is very little surface scattering. We obtain a very good fit with $\ln(\tau_\phi/$

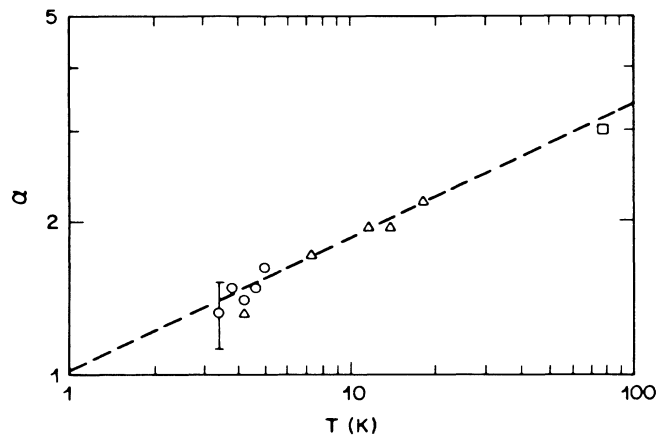


FIG. 4. The 3D fitting parameter α as a function of temperature from best fits to the data of Refs. 4 (circles), 21 (triangles), and 22 (square). The dashed line is a guide to the eye.

$\tau_0) \approx 5.6$. This value agrees favorably with that in Fig. 2 since one expects that configurational dephasing due to the perpendicular motion of the helium atoms may be less for larger $\langle z \rangle$. We conclude that the ^4He and H_2 data are consistent with the $\langle z \rangle$ dependence of Eq. (6).

We have also fitted 3D electron mobility data of other authors,^{21,22} at various temperatures between 4 and 77 K. Shown in Fig. 4 are the values of α obtained from the fits as functions of temperature. The small positive slope of α is not understood but may, in part, result from the momentum dependence of B_2 . At higher temperatures, the thermal wave vector of the electrons is larger and the k dependence of the ^4He pair-correlation function has to be taken into account, which is out of the scope of the present investigation.

In conclusion, we have measured the conductivity of 2D electrons in helium gas from which we have extracted a density-dependent conduction threshold, E_c . We present a model in which E_c is estimated by means of the weak-localization corrections to the conductivity and obtain very good one-parameter fits to both our data and the data of various authors with $E_c^{2D} \propto n_g$ and $E_c^{3D} \propto n_g^2$.

The authors wish to thank Dr. V. Elser, Dr. J. Jackson, Dr. D. Huse, Dr. M. Stephen, and Dr. S. Sachdev for helpful discussions.

¹This is essentially the Anderson criterion for strong localization. P. W. Anderson, *Phys. Rev.* **109**, 1492 (1958).

²J. L. Levine and T. M. Sanders, *Phys. Rev.* **154**, 138

(1967).

³W. T. Sommer and D. J. Tanner, *Phys. Rev. Lett.* **27**, 1345 (1971).

⁴K. W. Schwarz, *Phys. Rev. B* **21**, 5125 (1980).

⁵P. A. Lee and T. V. Ramakrishnan, *Rev. Mod. Phys.* **57**, 287 (1985).

⁶E. Abrahams, P. W. Anderson, D. C. Licciardello, and T. V. Ramakrishnan, *Phys. Rev. Lett.* **42**, 673 (1979).

⁷M. Saitoh, *J. Phys. Soc. Jpn.* **42**, 201 (1977).

⁸M. W. Cole and M. H. Cohen, *Phys. Rev. Lett.* **23**, 1238 (1969).

⁹P. W. Adams and M. A. Paalanen, *Phys. Rev. Lett.* **58**, 2106 (1987).

¹⁰T. R. Brown and C. C. Grimes, *Phys. Rev. Lett.* **29**, 1233 (1972).

¹¹Y. Iye, *J. Low Temp. Phys.* **40**, 441 (1980).

¹²K. Kajita and W. Sasaki, *Surf. Sci.* **113**, 419 (1982).

¹³T. P. Eggarter and M. H. Cohen, *Phys. Rev. Lett.* **25**, 807 (1970).

¹⁴S. Jackson, to be published.

¹⁵G. H. Watson, Jr., P. A. Fleury, and S. L. McCall, *Phys. Rev. Lett.* **58**, 945 (1987).

¹⁶M. Kaveh, D. J. Newson, D. Ben-Zimra, and M. Pepper, *Solid State Phys.* **20**, L19 (1987).

¹⁷G. Bergmann, *Phys. Rev. B* **28**, 2914 (1983).

¹⁸Our experiments could only be extended to $n_g \approx 10^{21} \text{ cm}^{-3}$ because of vanishing signal levels.

¹⁹P. W. Adams and M. A. Paalanen, to be published.

²⁰The data in Ref. 3 were scaled by a factor of 2 to give the proper zero-density limit; see Ref. 10.

²¹H. R. Harrison and B. E. Springett, *Phys. Lett.* **35A**, 73 (1971).

²²A. Bartels, *Appl. Phys.* **8**, 59 (1975).